

JAE-YEON KIM\*, JUNG-WOO HWANG\*\*, SEUNG-MI LEE\*\*, CHANG-YOUNG HYUN\*\*,  
IK-KEUN PARK\*\*\*, JAI-WON BYEON\*\*\*#

## EFFECT OF PROCESS VARIABLES ON FRICTION STIRRED MICROSTRUCTURE AND SURFACE HARDNESS OF AZ31 MAGNESIUM ALLOY

Effects of various friction stir processing (FSP) variables on the microstructural evolution and microhardness of the AZ31 magnesium alloy were investigated. The processing variables include rotational and travelling speed of the tool, kind of second phase (i.e., diamond,  $\text{Al}_2\text{O}_3$ , and  $\text{ZrO}_2$ ) and groove depth (i.e., volume fraction of second phase). Grain size, distribution of second phase particle, grain texture, and microhardness were analyzed as a function of the FSP process variables. The FSPed AZ31 composites fabricated with a high heat input condition showed the better dispersion of particle without macro defect. For all composite specimens, the grain size decreased and the microhardness increased regardless of the grooved depth compared with that of the FSPed AZ31 without strengthening particle, respectively. For the AZ31/diamond composite having a grain size of about 1  $\mu\text{m}$ , microhardness (i.e., about 108 Hv) was about two times higher than that of the matrix alloy (i.e., about 52 Hv). The effect of second phase particle on retardation of grain growth and resulting hardness increase was discussed.

*Keywords:* Friction stir process, AZ31 alloy, diamond particle, process variable, grain size

### 1. Introduction

AZ31 magnesium alloys have been investigated for the application of light structural components such as vehicle frame, sport goods, and case of electronic instrument due to their light weight and high specific strength. However, needs of surface hardening of the alloy are still exist because the alloy have little precipitates contributing to strength and mechanical durability. Out of surface modification techniques for Mg alloys such as, Friction Stir Processing (FSP) have attracted interest due to its merits of microstructural refinement and hardening by severe plastic deformation [1,2]. This process can be performed by travelling of rotating tool made by hard metal in soft metal specimen at room temperature.

Dispersion of various kinds of second phase particle to produce a composite structure near surface has been a big stream of this research [3-5]. The second phases particles dispersed in Mg alloy include CNT [3],  $\text{Al}_2\text{O}_3$  [4], SiC [5],  $\text{B}_4\text{C}$  [5], and so on. Very recently, a reactive-FSP utilizing in-situ phase formation during the FSP has been reported [6,7]. Although successful results of increasing surface strength have been documented [1-7], there is still a need of further hardening. In this research, the effect of kind and volume of the second phase including industrial diamond particle on the microstructural evolution and surface hardness was investigated.

### 2. Experimental

A rolled AZ31B-O Mg alloy (Magnesium Gurnee Metal Co. Ltd., China) was used for this study. The specimen size for FSP was 120 mm in length, 60 mm in width, and 6 mm in thickness. The chemical composition of the alloy was Mg: balance, Al: 2.5–3.5, Zn: 0.6-1.4, Mn: 0.2-1.0, Si: <0.1, Fe: <0.005, Cu: <0.04, and Ni: <0.005 mass %. The rotation tool made of SKD61 steel had a shoulder diameter of 16 mm, pin length of 4 mm, and pin diameter of 4 mm. The pin was designed with a screw-shape for improving stirring effectiveness. The stirring tool was tilted at a 3° forward angle from the vertical.

In order to study the effect of processing variable, a single-pass FSP was performed for the AZ31 specimen without particles at various conditions of a rotation speed (i.e., 715, 1000, and 1400 rpm) and of a travelling speed (i.e., 25, 95, 157, and 210 mm/min), respectively. To fabricate surface composites with different kind and fraction of strengthening phase,  $\text{Al}_2\text{O}_3$  powder (purity: 99.9 %, Size: <1  $\mu\text{m}$ ),  $\text{ZrO}_2$  powder (purity: 99.9%, size: 0.15-0.35  $\mu\text{m}$ ) and, industrial diamond powder (purity: 98%, size: 4-6 nm) was filled into a groove with different depth (i.e., width: 1 mm, depth: 2, 3, and 4 mm), respectively. Fig. 1 shows SEM images of the particles used in this study. The microstructure was analyzed by an Optical Microscope (OM), Scanning Electron Microscope (SEM) and X-ray Diffraction (XRD). The

\* SEOUL NATIONAL UNIVERSITY OF SCIENCE AND TECHNOLOGY, CONVERGENCE INSTITUTE OF BIOMEDICAL ENGINEERING AND BIOMATERIALS, PROGRAM OF MATERIALS SCIENCE & ENGINEERING, SEOUL, 01811, KOREA

\*\* SEOUL NATIONAL UNIVERSITY OF SCIENCE AND TECHNOLOGY, DEPARTMENT OF MATERIALS SCIENCE & ENGINEERING, SEOUL, 01811, KOREA

\*\*\* SEOUL NATIONAL UNIVERSITY OF SCIENCE AND TECHNOLOGY, DEPARTMENT OF MECHANICAL & AUTOMOTIVE ENGINEERING, SEOUL, 01811, KOREA

# Corresponding author: byeonjw@seoultech.ac.kr

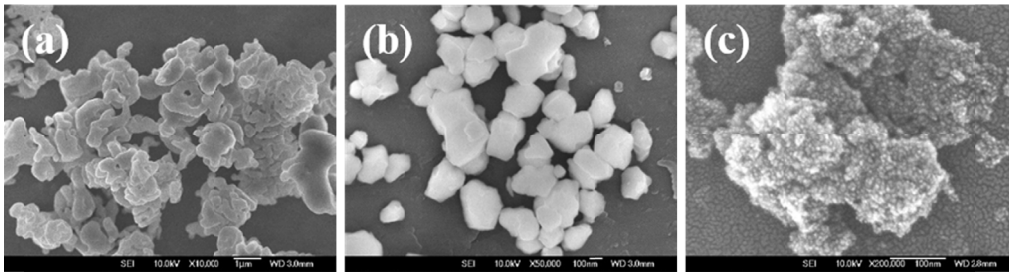


Fig. 1. SEM images of the particles used in this study: (a)  $\text{Al}_2\text{O}_3$ , (b)  $\text{ZrO}_2$ , and (c) diamond

Vickers hardness was measured on a cross-section of the stir zone under load of 100 g and for 15 seconds. Average grain size was measured by a line intercept method.

### 3. Results and discussion

Fig. 2(a-c) shows a typical optical microstructure of the FSPed specimens with no second phase fabricated at different travelling and rotational speed of the tool. Fig. 2(d) summarizes the change of grain size and microhardness in the stir zone as a function of tool travelling speed for the FSPed specimens at

various rotational speeds. Grain size was inversely proportional to the travelling speed at all rotational speeds investigated, which is because growth of the dynamically recrystallized grain was retarded due to relatively low heat input condition at high travelling speed [2].

Heat input during FSP can be calculated according to the following equation.

$$W = w^2 / v$$

where  $W$ ,  $w$ , and  $v$  are heat input, rotational speed (rpm) and travel speed (mm/min), respectively. Under the minimum heat input condition (i.e., 715 rpm, 215 mm/min, heat input:

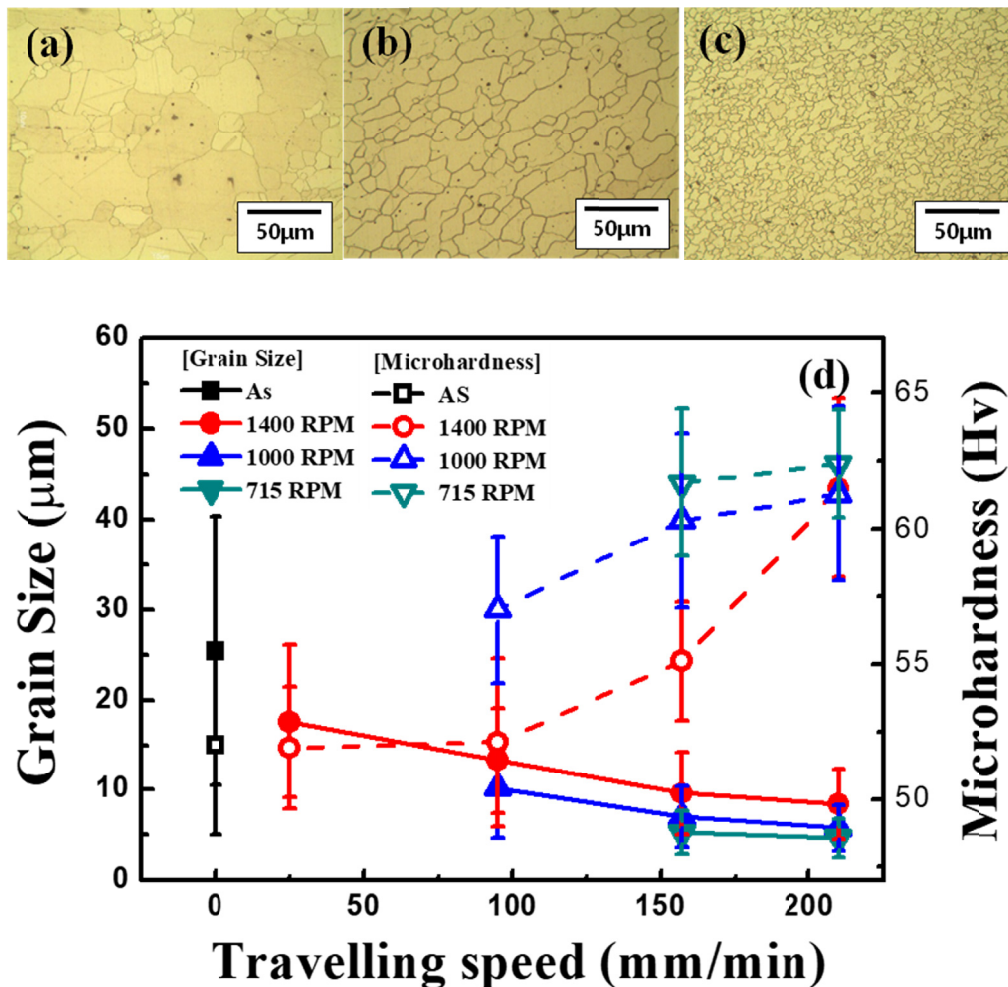


Fig. 2. Typical optical microstructure in the stir zone with rotational and travelling speed of the stirring tool: (a) as-received, (b) 1400 rpm, 25 mm/min, (c) 715 rpm, 210 mm/min., and (d) a summary of the grain size measured from these micrographs and microhardness in the stir zone

$2.4 \times 10^3 \text{ rpm}^2 \cdot \text{min}/\text{mm}$ ), grain size of about  $4.9 \mu\text{m}$  was obtained. The microhardness was roughly proportional to the travelling speed as a result of grain refinement.

Fig. 3 comparatively presents macro-images of surface and cross section of the FSPed AZ31/ $\text{Al}_2\text{O}_3$  specimens fabricated with a high heat input condition (i.e., 1400 rpm, 25 mm/min, heat input:  $7.8 \times 10^4 \text{ rpm}^2 \cdot \text{min}/\text{mm}$ ) and with a low heat input condition (i.e., 715 rpm, 210 mm/min, heat input:  $2.4 \times 10^3 \text{ rpm}^2 \cdot \text{min}/\text{mm}$ ). No macro defect was observed at high heat input condition, while several macro cavities formed under low heat input condition due to insufficient material flow [4,6].

Because insufficient heat input to generate macro defects is critically harmful for fabrication of bulk metallic components, a selection of high heat input condition is more preferable to achieve better dispersion without defect at the sacrifice of grain refinement of the composite.

In this experiment, all composites were fabricated at a high heat input condition (i.e., 1400 rpm, 25 mm/min). Fig. 4 shows SEM microstructure of the stir zone processed under 1400 rpm and 25 mm/min as a function of groove depth (i.e., volume fraction of the particle) and different second phases (i.e., diamond particle,  $\text{Al}_2\text{O}_3$ , and  $\text{ZrO}_2$ ). Volume fraction of the particle in the

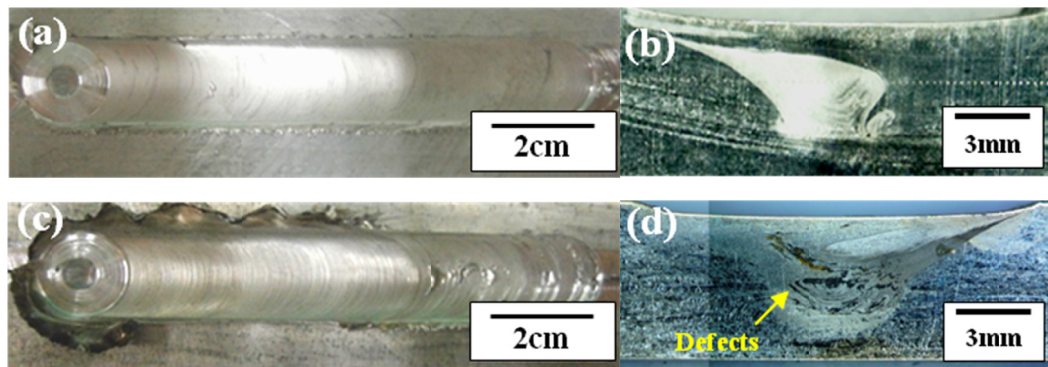


Fig. 3. Macro-images of surface and cross section of the FSPed AZ31/ $\text{Al}_2\text{O}_3$  specimens, respectively: (a, b) high heat input condition (i.e., 1400 rpm, 25 mm/min.) and (c,d) low heat input condition (i.e., 715 rpm, 210 mm/min)

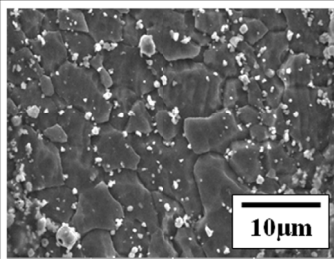
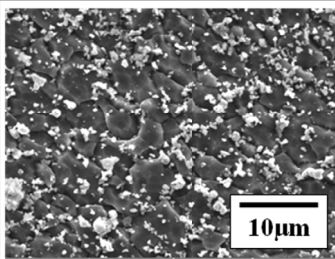
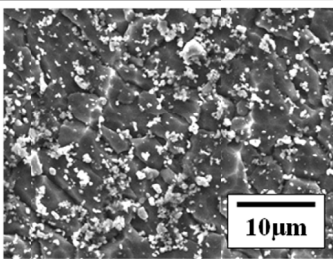
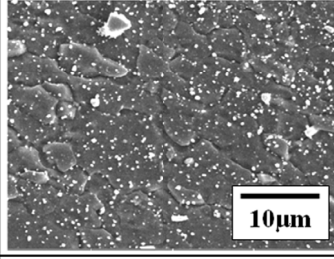
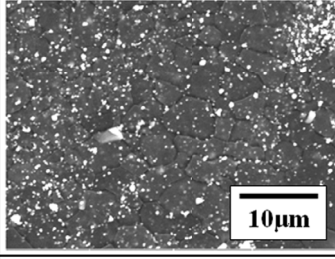
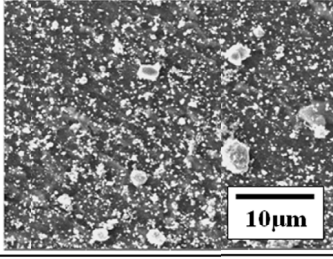
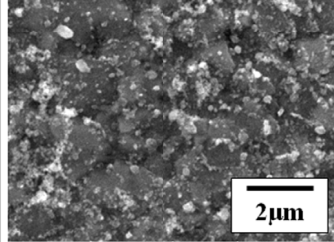
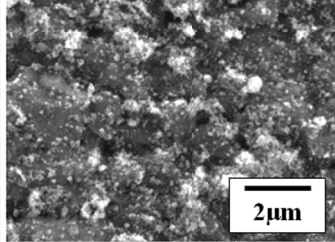
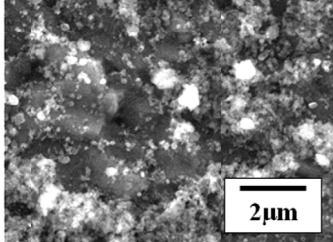
Particle Type	Groove Depth		
	2mm	3mm	4mm
$\text{Al}_2\text{O}_3$			
$\text{ZrO}_2$			
Dia			

Fig. 4. SEM microstructure of the stir zone processed under 1400 rpm and 25 mm/min condition as a function of different second phases (i.e.,  $\text{Al}_2\text{O}_3$ ,  $\text{ZrO}_2$ , and diamond particle) and with groove depth (i.e., volume fraction of the particle)

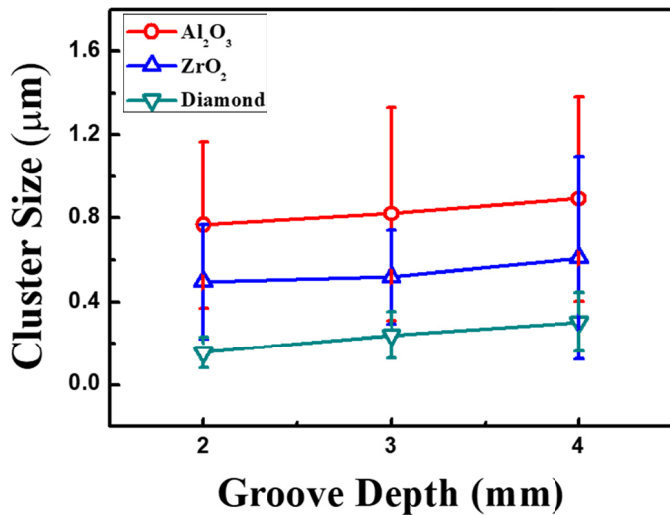


Fig. 5. Variation of cluster size measured in Fig. 4 with particle type and groove depth (i.e., volume fraction)

stir zone depends on the groove depth because the volume of stir zone is determined with tool size. Fig. 5 shows the distribution of agglomerated particles (i.e., cluster) size as a function of groove depth and type of particle. Together with homogeneously dispersed particles, agglomeration of the particles (i.e., cluster) was partly observed for all kinds of second phase particle for deeply grooved specimens, implying too much fraction of particles is difficult to homogeneously distribute under this process condition. Multi-pass process under medium heat input condition can be a solution to overcome the agglomeration without sacrificing grain refinement. The cluster size of FSPed AZ31/Diamond composite was remarkably reduced comparing with that of other composites, implying that the diamond of fine particle size (i.e., 4-6 nm) could be homogeneously distributed by FSP.

Fig. 6 presents the change of grain size of the composite specimens with various second phase and groove depth. Although the grain size decreased due to FSP for all composite specimens, too deep groove was not effective for refining grain

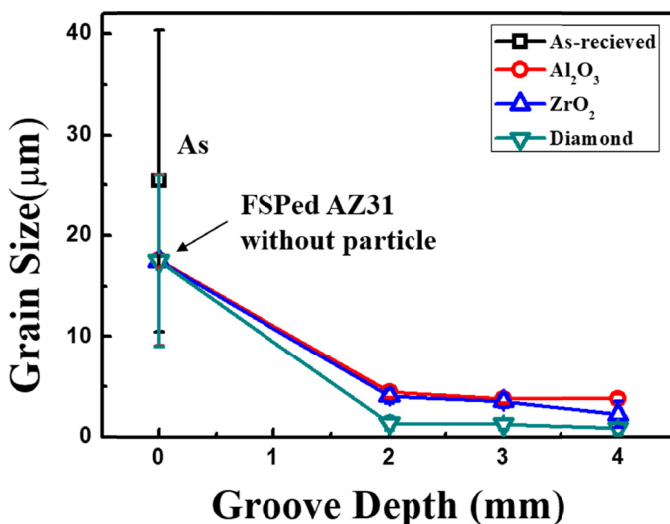


Fig. 6. Change of grain size of the composite specimens with various second phase and groove depth

size in a proportional manner. This saturation tendency of grain size is thought to be due to insufficient distribution of the high volume of second phase particle in the matrix. It is noted that the grain size was down to about 1 μm for the composite specimen with diamond particle. This grain refining behavior means the diamond particle used in this research effectively hindered grain growth because of their homogeneous distribution during the FSP as shown in Fig. 6.

Fig. 7(a) shows the variation of microhardness across the stir zone in the FSPed AZ31/Al<sub>2</sub>O<sub>3</sub> composite with different groove depth. Hardness in the stir zone was moderately homogeneous for all composite specimens and increased regardless of the groove depth. Fig. 7(b) compares the hardness among the specimens with different second phase particle in a groove depth of 2 mm. The highest hardness was observed for the FSPed specimen with diamond particles. The average hardness of this specimen (about 108 Hv) increased up to about 107% compared with that of the FSPed AZ31 without strengthening particle

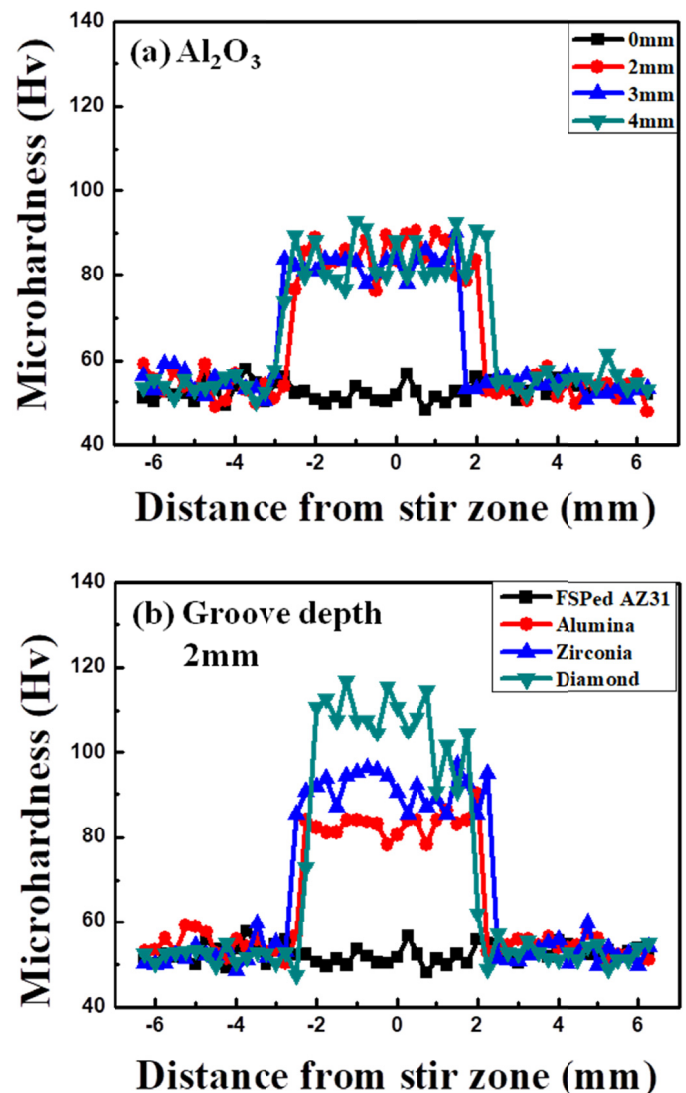


Fig. 7. Variation of microhardness across the stir zone: (a) FSPed AZ31/Al<sub>2</sub>O<sub>3</sub> composite with different groove depth and (b) FSPed composite specimens with different second phase particle in a groove depth of 2 mm

(52 Hv). The greatest increase in hardness of FSPed AZ31/diamond composite is attributed to grain refinement strengthening as shown in Fig. 6. On the other hand, dispersion strengthening is also effective for this strengthening due to the highest shear elastic modulus (diamond: 470 GPa,  $\text{Al}_2\text{O}_3$ : 165 GPa, and  $\text{ZrO}_2$ : 86.4 GPa) and the most homogeneous distribution (i.e., the smallest cluster size, Fig. 5) of diamond particle.

Fig. 8 comparatively presents X-ray diffraction pattern of the FSPed specimen with and without second phase particles. No in-situ reaction phase was detected in the X-ray diffraction results of all specimens analyzed. As-received specimen exhibited a strong (0002) peak, which is a typically developed texture in rolled-specimen. During the FSP, a (10 $\bar{1}$ 3) diffraction peak become prominent for the specimen without second phase, while (10 $\bar{1}$ 1) texture was dominantly developed in the specimen with second phase regardless of the type and volume of the particles. Considering that a development of crystallographic texture affects deformation properties such as elongation and formability, it needs to be further studied.

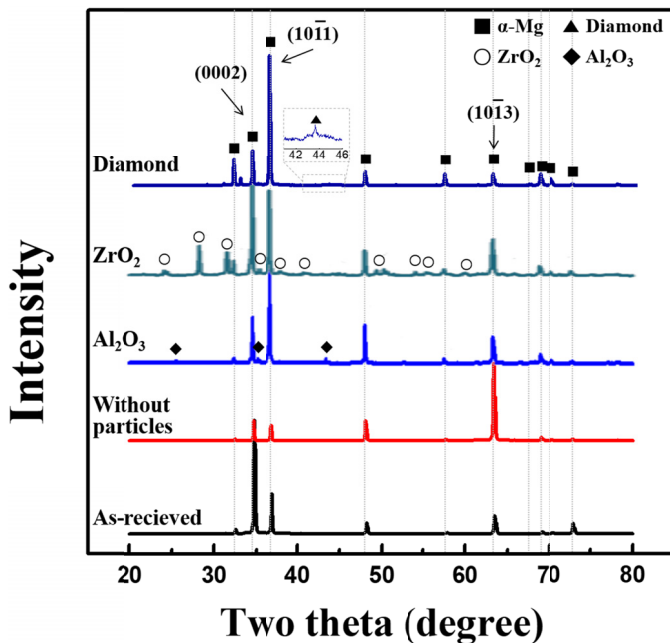


Fig. 8. X-ray diffraction patterns of the FSPed specimen with and without second phase particles

#### 4. Conclusions

Grain size of the FSPed specimen with no second phase was inversely proportional to the travelling speed of the tool. For all composite specimens, the grain size was reduced and the microhardness was improved regardless of the grooved depth compared with that of the FSPed AZ31 without strengthening particle, respectively. The FSPed specimen with diamond particle have an average grain size of about 1  $\mu\text{m}$  and the highest hardness of about 108 Hv among the second phase particles investigated. The hardness value obtained in this work was over two times higher than that of the FSPed matrix alloy (i.e., about 52 Hv). Different grain texture was developed depending on the absence and presence of the second phase, not depending on the type and volume fraction of the particle.

#### Acknowledgments

This work was supported by the Korea Institute of Energy Technology Evaluation and Planning (KETEP) and the Ministry of Trade, Industry & Energy (MOTIE) of the Republic of Korea (No. 20181510102130).

#### REFERENCES

- [1] W. Wen, W. Kuaishe, G. Qiang, W. Nan, *Rare Met. Mater. Eng.* **41** (9), 1522-1526, (2012).
- [2] J.A. Del Valle, P. Rey, D. Gesto, D. Verdera, J.A. Jimenez, O.A. Ruano, *Mater. Sci. Eng. A* **628**, 198-206, (2015).
- [3] J.Y. Kim, J.W. Hwang, H.Y. Kim, S.M. Lee, W.S. Jung, J.W. Byeon, *Arch. Metall. Mater.* **62**, 2B, 1039-1042, (2017).
- [4] M. Azizieh, A.H. Kokabi, P. Abachi, *Mater. Des.* **32**, 2034-2041 (2011).
- [5] G.M. Reddy, A.S. Rao, K.S. Rao, *Trans. Indian Inst. Met.* **66** (1), 13-24 (2013).
- [6] M. Azizieha, M. Mazaheri, Z. Balak, H. Kafashan, H.S Kim, *Mater. Sci. Eng. A* **712**, 655-662, (2018).
- [7] F. Khodabakhshi, A. Simchi, A.H. Kokabi, M. Sadeghahmadi, A.P. Gerlich, *Mater. Sci. Technol.* **31** (4), 426-435, (2015).